

DESIGNER COSMOLOGY

BRUCE A. BASSETT^{1,2}, DAVID PARKINSON² AND ROBERT C. NICHOL²¹ Department of Physics, Kyoto University, Kyoto, Japan and² Institute of Cosmology and Gravitation, University of Portsmouth, Portsmouth PO1 2EG, UK

Draft version June 15, 2018

ABSTRACT

The IPSO framework allows optimal design of experiments and surveys. We discuss the utility of IPSO with a simplified 10 parameter MCMC D-optimisation of a dark energy survey. The resulting optimal number of redshift bins is typically two or three, all situated at $z < 2$. By exploiting optimisation we show how the statistical power of the survey is significantly enhanced. Experiment design is aided by the richness of the figure of merit landscape which shows strong degeneracies, which means one can impose secondary optimisation criteria at little cost. For example, one may choose either to maximally test a single model (e.g. Λ CDM) or to get the best model-independent constraints possible (e.g. on a whole space of dark energy models). Such bifurcations point to a future where cosmological experiments become increasingly specialised and optimisation increasingly important.

Subject headings: cosmological parameters — large-scale structure of universe — surveys

1. INTRODUCTION

We have reached an enviable resonance in which improvements in detector performance and cost are allowing not only rapid gains in our fundamental knowledge of the cosmos but also the opportunity for smaller experiments to make critical contributions to that knowledge. This has resulted in a surge of interest in next-generation experiment design with over twenty major surveys in planning or construction in observational cosmology alone. Experimental cosmology has changed in a few short years into a crowded and jostling marketplace.

There are several big prizes currently at stake: *Detection of dark energy dynamics*, *B-mode polarisation and cosmological non-Gaussianity*. Competition, limited funding, low signal-to-noise and extreme competition mean that new surveys will need to be increasingly optimised to get the most out of them. The aims of this *Letter* are to show how this can be achieved in a cross-disciplinary way and to illustrate some of the rich aspects of cosmological optimisation.

2. IPSO

Integrated Parameter Space Optimisation (IPSO; Bassett 2004, hereafter B04) proceeds by first constructing a class of candidate survey/experiment geometries, S , labeled by survey parameters, s_i , such as areal and redshift coverage.

Second, a target parameter space, Θ , is defined, consisting of the parameters that we wish to optimally constrain (labeled $\theta_{\mu,\nu,\dots}$). There are also typically nuisance parameters we need to marginalise over (labeled $\varphi_{a,b,\dots}$).

Third, a Figure of Merit (FoM) is defined which assigns a single real number to each candidate survey. The candidate with the extremal FoM is the optimal experiment/survey. The FoM we consider is defined by (B04):

$$FoM(s_i) = \int_{\Theta} I(s_i, \vec{\theta}) p(\vec{\theta}) d\vec{\theta}. \quad (1)$$

$I(s_i, \vec{\theta})$ is a scalar which depends on the survey geometry (through the s_i), and position in Θ and $p(\vec{\theta})$ is a ‘window

function’ that weights the different regions of the parameter space. By integrating over the parameter space we do not make assumptions about the underlying model, which is particularly important when we have very limited knowledge of the underlying physics, as is the case with dark energy.

Most choices for $I(s_i, \vec{\theta})$ typically invoke either the parameter covariance matrix or \mathbf{F} , the Fisher matrix, defined by:

$$F_{AB} = - \left\langle \frac{\partial^2 \ln \mathcal{L}}{\partial \theta_A \partial \theta_B} \right\rangle = \sum_i \left(\frac{\partial X}{\partial \theta_A} \frac{\partial X}{\partial \theta_B} \right)_i \epsilon_i^{-2}(s). \quad (2)$$

Here we use $A = \{\mu, \dots, a, \dots\}$ to label both fundamental and nuisance parameters, \mathcal{L} is the likelihood, $X = C_\ell, d_L, H$ represents the quantity being measured with i labeling redshift bin or Fourier mode as appropriate (Tegmark *et al.* 1998). The ϵ_i^2 are the error variances on X and depend explicitly on the survey parameters, s_i , unlike the derivatives, $\partial X / \partial \theta_A$. In computing integrals such as (1) this allows for significant cpu gains since the derivatives need only to be computed once.

Via the Cramér-Rao bound \mathbf{F}^{-1} provides the best possible covariance matrix and hence a lower bound on the achievable parameter variances. Although there are many choices for $I(s_i, \theta_\mu)$ (B04) we focus on only one for simplicity: D-optimality, defined by

$$I(s, \theta_\mu) = \log \det(\mathbf{F} + \mathbf{P}) \quad \text{D-optimality} \quad (3)$$

where ‘det’ denotes matrix determinant and \mathbf{P} is the prior precision matrix, *viz.* the Fisher matrix of all the relevant prior data.

Eq. (3), is the gain in Shannon information or entropy over the prior. Maximising (3) provides the best possible gain in constraints on the parameters θ_μ over what was available from just the prior data, \mathbf{P} . It is known as D-optimality in the design literature. If $\mathbf{P} = 0$ maximising (3) is equivalent to minimising the volume of the error ellipses, an alternative FoM (Huterer and Turner 2001, Frieman *et al.* 2003, B04). Via the General Equivalence Theorem, D-Optimal solutions are also optimal under other FoM. For these reasons it seems appropriate for

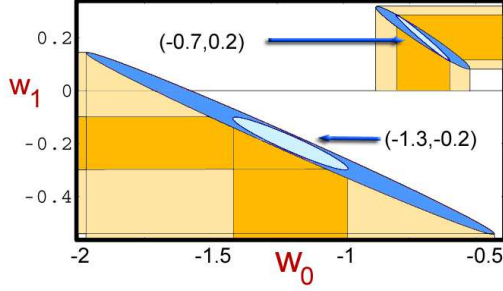


FIG. 1.— **Typical D-optimality improvements on error ellipses** at the two base points $(w_0, w_1) = (-1.3, -0.2)$ and $(-0.7, 0.2)$. The unoptimised survey (outer dark ellipses) has errors between 50% and three times larger in both w_0 and w_1 than the D-optimal survey (inner light ellipse) which was optimised around Λ CDM. Note the particularly significant gains in the phantom region $w_0 < -1$.

cosmological applications, although as we will see, secondary optimisation criteria can be imposed at almost no cost to the primary FoM.

Nuisance parameters, such as Ω_k, Ω_m etc..., whose values we do not know precisely but which we do not want to optimise with respect to, can be easily dealt with by inverting the full Fisher matrix F_{AB} , extracting the relevant submatrix corresponding to the θ_μ , re-inverting (e.g. Seo & Eisenstein 2003, B04) and then applying Eq. (3). Further, any reasonable FoM can also be generalised to allow inclusion of competing surveys by simply replacing $\mathbf{F} \rightarrow \mathbf{F} + \mathcal{F}$ where \mathcal{F} is the sum of the Fisher matrices expected for the competing surveys. In this way IPSO will find the optimal niche with respect to the other surveys (B04).

3. OPTIMIZING CMB AND WEAK LENSING SURVEYS

When is optimisation worth doing? To illustrate this let us contrast weak lensing (wl) convergence and CMB surveys on the celestial sphere. In both of these cases the Fisher matrix is a sum over ℓ (Hu and Tegmark 1999, Knox and Song 2002, Kesden *et al.* 2002):

$$F_{\mu\nu} = \sum_{\ell > f_{sky}^{-1/2}} \frac{2\ell + 1}{2} (N_\ell^X)^{-2} \frac{\partial C_\ell^X}{\partial \theta_\mu} \frac{\partial C_\ell^X}{\partial \theta_\nu} \quad (4)$$

where $X = CMB, wl$, N_ℓ^X is the total noise for the survey and f_{sky} is the fraction of the sky observed. For the CMB we consider only one spectrum (e.g. the B-mode power spectrum). In both cases we assume that the surveys are constrained to last a given length of time, T , and ask ‘what is the optimal sky coverage, f_{sky} , given this constraint?’ For CMB experiments we have (Knox 1995):

$$N_\ell^{CMB} \propto f_{sky}^{-1/2} (C_\ell^{CMB} + \frac{a f_{sky}}{T} e^{\ell^2 \sigma_b}) \quad (5)$$

where $T = t_{pix} N_{pix}$ is the length of the survey, a is a proportionality constant and the N_{pix} pixels are each observed for time t_{pix} using a Gaussian beam with $\text{FWHM} \propto \sigma_b$. The first (second) term in (5) is the noise from sample variance (instrument noise).

CMB experiments will benefit from optimisation since the competition between the terms in eq. (5) creates a

local minimum in the noise (Jaffe *et al* 1999). To apply IPSO to the CMB one must first choose Θ . For example, for optimal detection of deviations from the inflationary consistency conditions the key variable is $\theta \equiv n_t + r/4.8$ where n_t is the tensor spectral index and r is the ratio of tensor to scalar quadrupole in the CMB. Single field inflation predicts this should vanish. Hence a high- σ detection of $\theta \neq 0$ would put severe pressure on simple inflationary models. In contrast, an experiment designed to detect B-mode polarisation alone would optimise to detect r only and would lead to a different optimal area.

In contrast, for weak lensing (Kaiser 1992)

$$N_\ell^{wl} \simeq f_{sky}^{-1/2} C_\ell^{wl} + \frac{\sigma_g^2}{2\sqrt{T}\bar{n}} \quad (6)$$

where $\sigma_g^2 \sim 0.35$ is the approximately constant intrinsic ellipticity error and the surface density of detected galaxies scales roughly as $\bar{n}\sqrt{t}$ where t is the integration time per field of view. The noise terms N_ℓ^X differ crucially when it comes to optimisation of the areal coverage, f_{sky} . Unlike the CMB noise, N_ℓ^{wl} has no local minimum; the weak lensing Fisher matrix is a monotonic function of f_{sky} . Optimising any of the FoM simply proceeds by using the largest feasible area to minimise the sample variance.

If, in addition, the intrinsic ellipticity noise dominates the noise (as it does for the proposed SNAP WAS) then the FoM becomes essentially independent of f_{sky} and the gain of going to the largest area is minimal, as found by (Rhodes *et al.*, 2004).

4. OPTIMAL MEASUREMENTS OF THE HUBBLE CONSTANT

To illustrate some of the issues one faces in applying IPSO to realistic surveys, consider the optimisation of a redshift survey designed to measure the Hubble constant through observation of the radial baryon oscillations (Seo & Eisenstein 2003, Blake & Glazebrook 2003, Linder 2003, Amendola *et al.* 2004, Yamamoto *et al.* 2005). For clarity we assume no nuisance parameters, a flat FLRW model with $\Omega_m = 0.3$, H_0 known exactly and we ignore the constraints from d_A which a full optimisation would include.

We consider a model of dark energy based on Taylor expansion in powers of $(1 - a) = \frac{z}{1+z}$ (Chevallier M., Polarski 2001, Linder 2003, Bassett, Corasaniti & Kunz 2004), with $w = p_{DE}/\rho_{DE}$

$$w(z) = w_0 + w_1 \frac{z}{1+z} + w_2 \frac{z^2}{(1+z)^2} \\ \rho_{DE} \propto (1+z)^{3(1+w_0+w_1+w_2)} \times \\ \exp\left(\frac{-3z(2w_1(1+z) + w_2(2+3z))}{2(1+z)^2}\right) \quad (7)$$

where $\rho_{DE}(z)$ is the dark energy energy density.

Comparing with eq. (2), $X = E \equiv H/H_0$. Rather than the optimal area, f_{sky} , we want the optimal number of redshift bins, N , what redshifts they should be centered on, z_i , and how long we should observe in each bin, t_i . Again we assume fixed total survey time (T) so we need to optimise given the constraint $\sum_i^N t_i = T$.

We assume that the error bars scale as $\epsilon_i^{-2} = e_i t^\gamma$ where $e_i \propto (1+z_i)^{-\beta}$ gives the efficiency with which

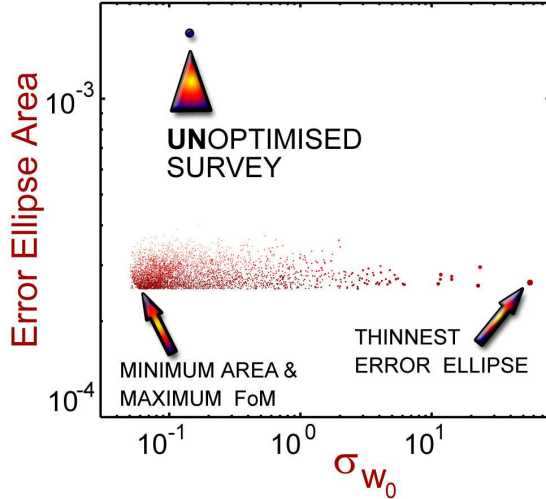


FIG. 2.— **Error on w_0 (σ_{w_0}) versus area of the error ellipse.** Note the wide range of σ_{w_0} at almost constant minimum area. σ_{w_0} effectively measures the ellipticity of the error ellipse. At nearly constant FoM one can optimise to obtain circular or very thin ellipses, depending on one’s aims. The size of the points is proportional to the error in w_1 .

galaxies are detected and γ, β parameterise our ignorance. These could be treated as nuisance parameters to be marginalised over but we find that our main results are insensitive to both over the range $\beta = 1 - 2, \gamma = 1 - 2$ we consider. Note that $\gamma = 1$ implies that the FoM is maximised on the boundary of the allowed redshift region (just as was the case with the weak lensing survey earlier). We focus on the case $\gamma = 2$ here for illustrative purposes. The real constraint will be significantly more complex and we leave this issue to future work.

We restrict the bin redshifts to be between $0.5 < z_i < 4.5$ which is a feasible range for future baryon oscillation surveys such as KAOS and set $w_2 = 0$ for clarity. We performed an MCMC (Christensen and Meyer, 2000) optimisation with the D-Optimal FoM (3) with ten free survey parameters: $\{t_i, z_i\}$ giving the integration time and redshifts of the five bins. The effective number of bins varies dynamically because the MCMC chain could (and typically did) assign negligible amounts of observing time to some of the bins.

We ran multiple chains (up to 5000) with random starting configurations for the survey and used a standard Hastings-Metropolis algorithm for jump acceptance. Instead of directly performing the integral (1) we used the definition $FoM(s) = \frac{1}{N} \sum_{i=1}^N I(s, \theta_a)$ where the θ_a are drawn randomly from a probability distribution based on $p(\theta_i)$ in (1). We chose p to be a bi-variate Gaussian centered on the Λ CDM point $w_0 = -1, w_1 = 0$ so our optimisation was chosen to detect slowly varying dark energy dynamics close to a cosmological constant.

The Fisher matrix derivatives based on eq. (7) are simple to compute; e.g.

$$\begin{aligned} \frac{\partial \rho_{DE}}{\partial w_0} &= 3\rho_{DE} \ln(1+z) \\ \frac{\partial \rho_{DE}}{\partial w_1} &= 3\rho_{DE} \left(\ln(1+z) - \frac{z}{1+z} \right). \end{aligned} \quad (8)$$

Our unoptimised fiducial survey had five redshift bins

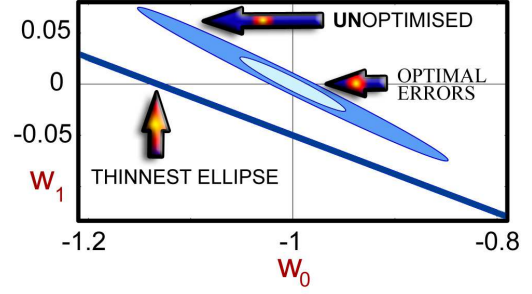


FIG. 3.— **Choices in optimisation.** At constant FoM one can optimise to achieve thin error ellipses with tiny transverse errors (diagonal dark blue “strip”) or to achieve the best joint constraints on all parameters (light blue ellipse). All ellipses are computed at $w_0 = -1, w_1 = 0$ and reduce the total unoptimised ellipse area (dark blue ellipse) by about 600%.

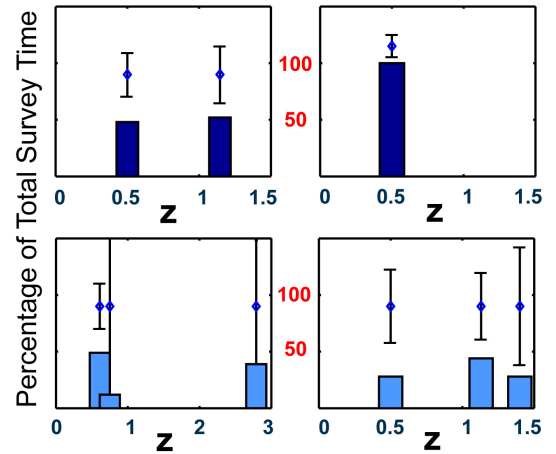


FIG. 4.— **Redshifts and integration times for the optimal surveys shown in Fig. (2) and the resulting error bars on $H(z)$.** **Top Left** - D-optimal maximum FoM (which also has the minimum error ellipse area). It splits the total survey equally between $z = 0.5$ and $z = 1.15$. **Top Right** - the thinnest possible ellipse with all measurements at a single redshift, $z = 0.5$. The **bottom two panels** show the geometries for the 2nd (left) and 2000th (right) largest FoM (only 0.005% and 6% smaller than the maximum respectively). This shows the diversity of geometries with nearly degenerate FoM.

located at $z_i = 0.6, 0.8, 1, 1.2, 3$, as in (Seo & Eisenstein 2003 and Amendola *et al.* 2004), with equal integration time ($T/5$) assigned to each bin.

Fig. (1) shows typical gains over the unoptimised survey for a near optimal survey chosen randomly from the 5000 MCMC chains while Fig. (2) shows the area of the error ellipse versus the corresponding error on w_0 for each of the 5000 locally optimal solutions. It is very clear that at almost identical area (and FoM) there is a very wide range of error ellipse ellipticity (controlled by σ_{w_0}). In other words, there are many local maxima which come very close to matching the global maximum.

The implications of this FoM ‘degeneracy’ for ruling out dark energy models are clarified in Fig. (3) where we show the thinnest error ellipse (diagonal “strip”), the unoptimised error ellipse and the error ellipse with the maximal FoM, all computed at the Λ CDM point (the thinnest ellipse is shifted down for clarity).

This degeneracy offers the chance for secondary opti-

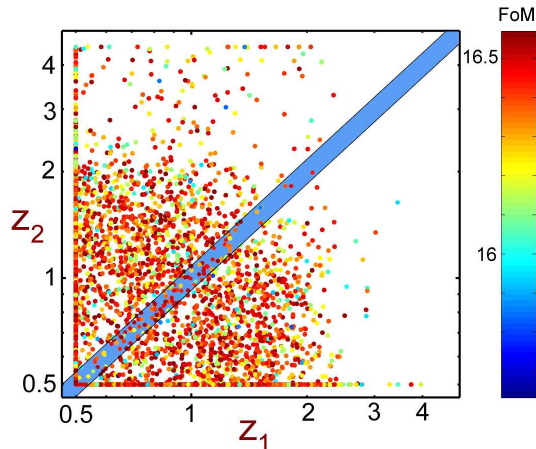


FIG. 5.— Phase plot of the redshifts, z_1, z_2 , of the two dominant bins with the most integration time for 5000 separate MCMC optimisation chains. The dominant bins are typically found at $z_{1,2} < 2$ although surveys with $z_2 > 2$ can be competitive. Note the clustering around the minimum redshift we considered, $z = 0.5$. The diagonal band results in very thin error ellipse (large σ_{w_0} in figure (2)).

misation (the primary one in this case being based on the D-optimal FoM). For example, one could choose geometries that deliver the best constraints on a particular linear combination of the parameters θ_μ adapted to the degeneracy structure of the observations while sacrificing the orthogonal direction(s). This amounts to minimising the smallest eigenvalue of the covariance matrix which may be preferable for testing dark energy dynamics in the short term.

The redshifts, z_i , and integration times, t_i , for each bin of some optimal and near optimal surveys are shown in Fig. (4) along with corresponding error bars on the Hubble rate, $H(z)$. Typically the locally optimal geometries in our 5000 chains had only two (51% of all chains) or three redshift bins (39% of all chains) with more than 5% of the total survey time. Optimal geometries with either one or five bins were extremely rare, forming less than 1% of all the locally optimal geometries (although single bin geometries deliver the thinnest error ellipses). The preference for only a few bins arises because the dark energy models we consider vary rather slowly with redshift,

hence it is statistically preferable to constrain w rather than dw/dz . This conclusion may change somewhat if one allows very rapid evolution in $w(z)$ which actually provides a very good fit to current SNIa data (Bassett *et al.*, 2004). We found that the redshifts of the two bins with the most integration time were typically located at $z < 2$ (as shown in Fig. (5)).

5. CONCLUSIONS

We have considered optimisation both of 2-d surveys such as CMB and weak lensing experiments and 3-d redshift surveys. In a simplified optimisation of a baryon oscillation survey we have shown how IPSO allows significant gains in the statistical power of a survey can be achieved through optimisation, in this case a reduction by a factor of 6 in the error ellipse area over the unoptimised survey. We found that there are many diverse surveys with nearly degenerate figures of merit (FoM), as shown in Figs. (4) & (2). This is good news since it allows survey designers to pick a near optimal survey structure that is most compatible with real-world intangibles that cannot easily be included explicitly in the optimisation.

The Monte Carlo Markov Chain (MCMC) search was repeated thousands of times with randomly chosen initial survey configurations. Most of the resulting locally optimal surveys divided $> 90\%$ of the survey time between only two or three redshift bins. A single bin leads to the thinnest possible error ellipse and may be appropriate for some experiments, particularly if the resulting ellipse is orthogonal to those coming from other observations. Alternatively, at almost the same FoM, one can choose a survey configuration that gives the best joint constraints on all the parameters simultaneously. At least for measurements of the Hubble constant alone, we found that typically the two dominant redshift bins should be located at low redshift, $z < 2$, as shown in Figures (4) and (5). This is good news for upcoming baryon oscillation surveys such as KAOS which will be able to probe the optical region $z < 1.3$ with high precision from earth.

We thank Chris Blake, Eric Linder and Takahiro Tanaka for useful comments on the draft.

REFERENCES

- Amendola L., Quercellini C. and Giallongo E., preprint (astro-ph/0404599).
- Bassett B. A., 2004, preprint (astro-ph/0407201), (B04)
- Bassett B. A., Corasaniti P. S., Kunz M., 2004, preprint (astro-ph/0407364)
- Blake C., Glazebrook K., 2003, ApJ, **594**, 665
- Chevallier M., Polarski D., 2001, IJMPD, **10**, 213
- Christensen N., and Meyer R., 2000, preprint (astro-ph/0006401).
- Frieman, J. A., Huterer D., Linder E. V. and Turner M. S., 2003, Phys. Rev. D **67**, 083505.
- Hu W., and Tegmark M., 1999, ApJ **514**, L65.
- Huterer D., Turner M., 2001, Phys Rev D **64**, 123527.
- Jaffe A.H., Kamionkowski M., and Wang, L., 2000, Phys. Rev. D **61**, 083501
- Jungman G., Kamionkowski M., Kosowsky A., Spergel D. N., 1996, Phys Rev D **54**, 1332.
- Kaiser, N. 1992, ApJ, **388**, 272
- Kesden, M., Cooray, A., and Kamionkowski, M., 2002, Phys. Rev. Lett. **89**, 011304.
- Knox, L., 1995, Phys. Rev. D **52**, 4307.
- Knox, L., and Song Y-S., 2002, Phys.Rev.Lett. **89** 011303
- Linder E. V., 2003, Phys. Rev. Lett, **90**, 091301
- Linder E. V., 2003, Phys. Rev. D **68**, 083504 (2003)
- Magueijo J., Hobson M. P., 1997, Phys. Rev. D, **56**, 1908.
- Refregier A., *et al.*, 2003, preprint (astro-ph/0304419)
- Rhodes J., Refregier A., Massey R., [the SNAP Collaboration], Astropart. Phys. **20** (2004) 377
- Seo H. J., Eisenstein D. J., 2003, ApJ, **598**, 720
- Tegmark M., Eisenstein D. J., Hu W., Kron R., 1998, preprint (astro-ph/9805117)
- Tegmark M., Taylor A. and Heavens A., 1997 ApJ, **480**, 22
- Tegmark M., 1997, Phys. Rev. D, **56**, 4514
- White M. J., Carlstrom J., Dragovan M. and Holzapfel S. W. L., 1999, preprint (astro-ph/9912422).
- Yamamoto, K., Bassett, B. A., and Nishioka, H., 2005, Phys. Rev. Lett. **94**, 051301